

LOW-SPEED WIND TUNNEL IMPROVEMENTS AT THE UNIVERSITY OF NORTH FLORIDA

William J. Harrington
University of Florida
Gainesville, Florida, USA

James H. Fletcher
University of North Florida
Jacksonville, Florida, USA

Joseph L. Campbell
University of North Florida
Jacksonville, Florida, USA

ABSTRACT

The University of North Florida Mechanical Engineering Department currently uses a low speed suction type wind tunnel for pedagogical and research experiments. Wind tunnel experiments range from airfoil and coefficient of drag analysis to convection studies.

The wind tunnel was designed and assembled by mechanical engineering students in the spring of 2003 and originally outfitted with a 2-horsepower blower. With this configuration, the wind tunnel achieved test section Mach numbers of 0.15. Due to the demand for higher Mach number testing, the wind tunnel was upgraded to attain test section Mach numbers of 0.30. In addition to a larger blower, considerable flow transitions were added to improve flow quality and reduce losses within the wind tunnel.

WIND TUNNEL DESCRIPTION

The wind tunnel at the University of North Florida was designed and built by mechanical engineering students in the spring of 2003. The suction type wind tunnel is approximately 18-ft long with an 8-in square test section. The wind tunnel was constructed from 16-gauge sheet metal and built on two moveable wooden frames.



Figure 1. Wind tunnel schematic

The wind tunnel can be divided into five distinct sections as seen in Figure 1. The first section is the bell-mouth where the air is drawn into the wind tunnel. The second section is a straight section with a 16-in square cross-section where the air is conditioned using tube flow straighteners. The third section is the converging section where the inner width of the wind tunnel is brought from 16-in to 8-in., maintaining the square cross-section. After passing through section three, the air passes through a constant area test section and then through the diffuser at section four. The diffuser is for pressure recovery; the velocity is decreased in order to recover some of the velocity head into pressure head. After passing through the diffuser at section four, the air passes through another straight section at section five before entering the blower. In the discussion that follows, the paper will reference each of these sections with its designated section number.

The wind tunnel was originally outfitted with a 2-horsepower electric blower from American Coolair as seen in Figure 2. This blower assembly recovered 1.7-in of water at maximum output and enabled the wind tunnel to produce test section Mach numbers up to 0.15. During experiments where the blower was operating at maximum design speed, the flow quality would suffer. At high operating speeds the test section velocity would fluctuate as much as 10%. This surging effect would occur because the blower motor could not maintain a constant speed when operating under full load conditions. This decreased the repeatability of data that was recorded in the test section when running lab experiments at maximum speed.



Figure 2. Original wind tunnel blower

The wind tunnel also incorporates two flow conditioners. Upstream of the test section located in section 2 are 256 1-in diameter aluminum tubes. They ensure that the air entering the wind tunnel has been aligned and large, low spatial frequency turbulence is minimized. Second, a wire mesh is located in section 5 of the wind tunnel in order to reduce the amount of turbulence that would travel upstream from the blower.

WIND TUNNEL IMPROVEMENT GOALS

The upgraded wind tunnel needed to operate at a test section velocity twice that of the old wind tunnel. An appropriate blower had to be sized for a test section Mach number of 0.30. In order to reduce the amount of resources required for wind tunnel operation, all losses within the wind tunnel needed to be minimized. Improving wind tunnel performance included enhancing transition areas and sealing all leaks within the wind tunnel.

WIND TUNNEL CALCULATIONS

In order to determine the proper size blower for wind tunnel operation at a test section Mach numbers of 0.30, the wind tunnel losses were calculated. Prior operation of the wind tunnel at lower speeds revealed the magnitude of pressure drop across the bell-mouth relative to the total pressure drop is minuscule. Therefore, the assumption that the losses inside the bell-mouth of section 1 were negligible due to the low velocity flow from the large section area. The losses for the test section, section two, and section five were all calculated using the same method due to their similar geometry. For the straight sections, it was assumed that the losses

generated in the viscous region could be calculated from turbulent flat-plate theory.

White [1] defines the coefficient of drag for turbulent flat-plate flow below the fully rough regime in Equation 1. With the coefficient of drag known, the losses can be calculated from Equation 2.

$$C_D = 0.031 \cdot \text{Re}_L^{-1/7} \quad (1)$$

$$h_f = \frac{1}{2} \cdot \rho \cdot C_D \cdot U_\infty^2 \quad (2)$$

The losses in the contraction nozzle located in section three were calculated from an approximation for the loss coefficient given by Wattendorf as Equation 3 [2]. This loss coefficient was used in conjunction with Equation 4 [2] to determine the losses through the nozzle.

$$K_{nt} = 0.32 \cdot f_{av} \cdot L_n \cdot D_{ts}^{-1} \quad (3)$$

$$h_f = \frac{1}{2} \cdot K_{nt} \cdot V^2 \cdot g^{-1} \quad (4)$$

Finally, the losses in the diffuser of the wind tunnel were calculated. The purpose of the diffuser is to recover the static pressure inside the wind tunnel. This process must occur with minimal flow separation to reduce the amount of pressure the blower must recover. The loss coefficient for the diffuser can be decomposed into the sum of a frictional loss coefficient and an expansion loss coefficient. The frictional loss coefficient is quite straightforward as suggested by Pope [2] in Equation 5.

$$K_f = \left(1 - \frac{1}{A_R^2}\right) \cdot \frac{f}{8 \cdot \sin \theta} \quad (5)$$

$$K_{ex} = K_e(\theta) \cdot \left(\frac{A_R - 1}{A_R}\right)^2 \quad (6)$$

The expansion loss coefficient is a function of both the conical angle and the area ratio of the diffuser as listed in Equation 6 [2]. The portion of the equation that is based on the conical angle is based primarily on experimental data collected by Eckert [3]. The empirical data is represented in Equation 7.

$$K_e(\theta) = -0.01322 + 0.05866 \cdot \theta \quad (7)$$

The results from the wind tunnel calculations have been tabulated in Table 1. The

losses through the diffuser contribute nearly 90% of the total losses in the wind tunnel at a test section Mach number of 0.30.

Table 1. Summary of wind tunnel losses

Section #	Frictional Losses (inches of H ₂ O)	Percentage of Total Losses (%)
2	0.006	0.08
3	0.715	9.86
Test Section	0.090	1.31
4	6.433	88.73
5	0.003	0.03
Total	7.247	100

With the total losses known, a blower could be selected. At a test section Mach number of 0.30, the volumetric flow rate through the wind tunnel is 9,100-cfm. With assistance from American Coolair, the VSAC24 was selected as the blower for the wind tunnel. As shown in Figure 3, at 9,100-CFM the blower will be more than sufficient at recovering the required 7.25-in of H₂O with a suction pressure of 8.5-in of H₂O.

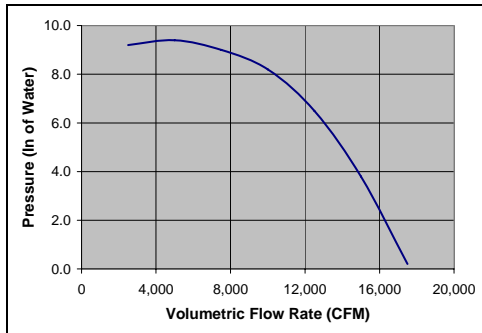


Figure 3. Fan curve for VSAC24 blower

WIND TUNNEL IMPROVEMENTS

In addition to upgrading the blower, many improvements were made to other areas of the wind tunnel. Improvements include the redesign of the entrance and exit of the test section, improved flow conditioners, elimination of leaks in the wind tunnel, the addition of a transition area for the blower and data acquisition system.

The wind tunnel has been configured to accept multiple test section lengths, and therefore must facilitate test section removal and installation. Originally the test section was joined to the uneven welded surface at the exit of section three and inlet of section four. This uneven transition from the test section to the wind tunnel introduced undesirable turbulence

and leaks. The uneven ends of the wind tunnel were replaced with wooden inserts in order to create a flush transition from the test section to the wind tunnel. The wooden inserts are displayed in Figure 4. Epoxy body filler was added to the inserts to produce a seamless transition from the wind tunnel to the wooden inserts.

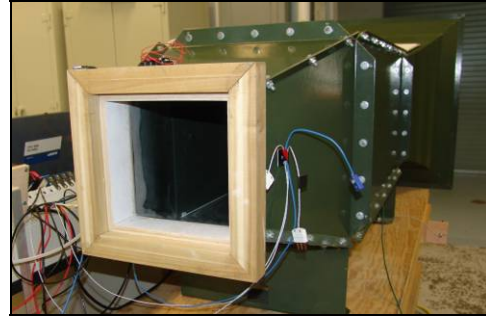


Figure 4. Test section transition inserts

The flow conditioners are located at the beginning of the wind tunnel in section two. Each of these 1-in diameter aluminum tubes were cut using an industrial saw. The saw provided a rapid cut, but left the edges tapered and with burrs. These burrs can introduce undesirable flow irregularities. The flow straighteners were removed from the wind tunnel and re-cut on a band saw and polished in order to create a sharp, clean edge. The end of an unfinished and finished tube is shown in Figure 5.

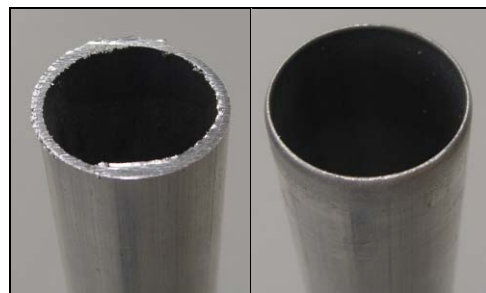


Figure 5. Difference between unfinished and finished tube flow straighteners

The wind tunnel was created from multiple sheet metal sections that were bolted together at the seams. During assembly, silicone caulk was applied to the seams of the wind tunnel sections to reduce the amount of leaks. Because the wind tunnel operates at a pressure less than atmospheric, areas that were inadvertently left unsealed allowed air to infiltrate from the sides. Leaks produce detrimental flow entries that can

disturb flow paths and decrease wind tunnel performance. The solution to fix the leaks on the wind tunnel was to force silicone caulk into the untreated areas while the wind tunnel was operating. The suction from the wind tunnel drew the silicone into all untreated areas.

Finally, the wind tunnel needed to be modified to accommodate the considerably larger blower. The exit of the wind tunnel is a 21-in square duct while the entrance of the blower is a 24.5-in diameter round duct. An adapter plate was fabricated to allow for the wind tunnel to be coupled to the blower. Included in the adapter plate are four triangular inserts that allow for a smooth transition from the square duct of the wind tunnel to the round duct of the blower. Epoxy body filler was added to the wooded inserts to create a seamless transition as shown in Figure 6.

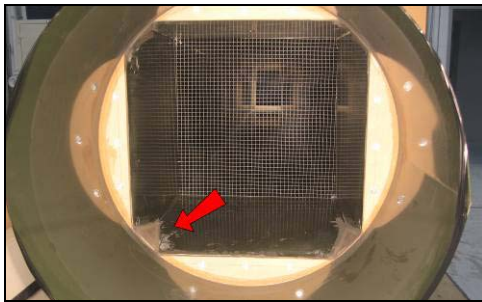


Figure 6. Wind tunnel with wooden inserts highlighted by arrow

A data acquisition system was acquired in order to meet the variety of wind tunnel testing planned. The data acquisition system records data collected by a National Instruments 9172 CompactDAQ chassis in conjunction with a NI 9201 voltage module, NI 9211 thermocouple module, and 9217 RTD module. In addition to the three analog input modules, a NI 9481 SPST relay module was used for digital control.

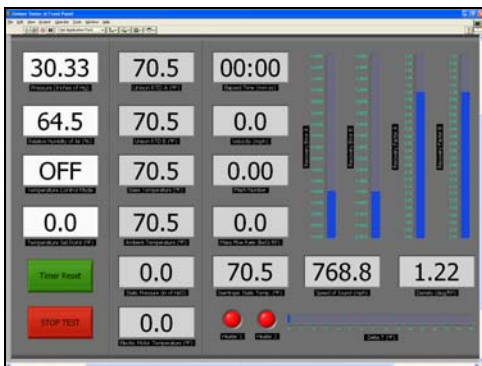


Figure 7. Screenshot of LabVIEW interface

The ambient temperature is measured using a 100 Ω resistance temperature detector (RTD) placed near the bell-mouth where the reference velocity is negligible. The test section velocity is correlated to a static pressure measured from section two using an Omega PX653-03D5V differential pressure transducer. Section two is an ideal location for measuring static pressure due to its relatively uniform and steady velocity profile. A custom LabVIEW interface was created to record and view data as seen in Figure 7. The relative humidity and barometric pressure are manually entered into the LabVIEW program at the beginning of each test. The relative humidity is measured using an Omega HH310 hygrometer while the barometric pressure was measured using a Princo 469 Nova barometer. Data acquisition hardware enabled fast, reliable, data measurement over a variety of experiments. Figure 8 is an example of how data acquisition was configured and used to take measurements from a total temperature sensor.

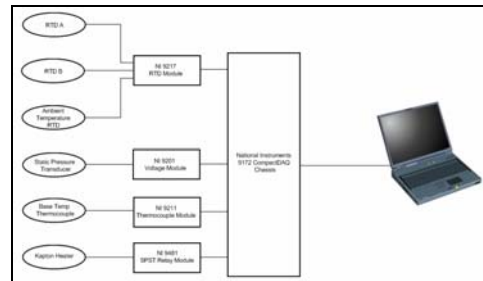


Figure 8. Data acquisition configuration for total temperature sensor

WIND TUNNEL TESTING AND RESULTS

After joining the new blower to the existing wind tunnel assembly, the wind tunnel was ready for testing. The velocity inside the wind tunnel was calculated from differential pressure measurements using a Pitot tube and the Pitot formula listed. Equation 8 can be used assuming the flow is brought to rest isentropically through the Pitot tube. The Pitot tube was inserted into the center of the flow, and the static and stagnation pressures were measured using a differential pressure transducer. A maximum differential pressure of 26-in of H₂O was measured at the test section.

$$V = \left[2 \cdot \frac{(p_o - p_s)}{\rho} \right]^{1/2} \quad (8)$$

The maximum velocity measured by the Pitot tube in the test section was 230-mph. With the air conditions of the room taken into consideration, the test section Mach number is 0.32. At a Mach number of 0.32, the wind tunnel blower was unable to maintain steady flow conditions due to surging. In order to generate a flow that is surge-free, the blower was run at the value necessary to produce a maximum test section Mach number of 0.30.

The losses from the wind tunnel were measured using the stagnation pressure port of the Pitot tube. The Pitot tube was placed at the end of the wind tunnel near the blower to measure the total pressure loss through the wind tunnel. The maximum pressure loss recorded throughout the wind tunnel at a test section Mach number of 0.30 was approximately 6.25-in of H₂O. Compared to the 7.25-in of H₂O calculated previously, the measured value is 14% less than the predicted value.

DISCUSSION

As seen in the wind tunnel test results shown in Figure 9, the measured losses were less than the calculated values. When comparing the pressure drop in section four of the wind tunnel with the calculated losses, the source of disparity becomes apparent. The loss measured in section four was approximately 5.7-in of H₂O while the calculated value was 6.4-in of H₂O. The losses in section four are less than that of the calculated values primarily because the contribution due to flow separation was less severe than anticipated by the empirical data suggested by Eckert.

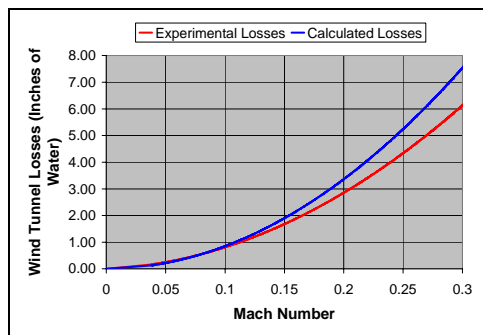


Figure 9. Comparison of calculated and measured losses vs. Mach number

During extended periods of wind tunnel testing the ambient room temperature would increase by 5-6°F. This was due to the cumulative energy that the bower was adding to the room air and the energy dissipated by the electrical motor due to efficiency loss. Even with

a 90% efficiency, the electrical motor generates 1.5-kW of heat power. The changes in air temperature create sources of error in measurement and decrease repeatability of lab experiments.

There also was a noticeable reduction in blower performance during prolonged experiments. Instead of reaching a maximum test section Mach number of 0.32-0.31, the blower would only reach Mach numbers of 0.29-.28. As the temperature of the motor would increase, the motor efficiency would decrease causing a reduction in blower output.



Figure 10. Insulated box for cooling electrical motor

The solution for the increase of ambient room temperature and motor efficiency are shown in Figure 10. The electrical motor was encased in an insulated box with two radiators. The two radiators were supplied with chilled water and the radiators would blow cold air across the fins of the electrical motor. This resulted in a 60% decrease in the ambient room temperature rise.

CONCLUSION

In closing, the wind tunnel was successfully upgraded to produce and maintain test section Mach numbers of 0.30. This was accomplished through extensive flow calculations and the successful implementation of these calculations through the use of an upgraded blower, improved flow transition areas, and the reduction of leaks within the wind tunnel. In addition, the University of North Florida has expanded its research capabilities through a more robust wind tunnel and data acquisition system.

REFERENCES

- [1] White, F., 2008, *Fluid Mechanics*, McGraw-Hill, New York, pp. 465-467, Chap. 7.
- [2] Barlow, J., Rae, W., Pope, A., 1999, *Low-Speed Wind Tunnel Testing*, Wiley, New York, pp. 70-102, Chap. 3.
- [3] Eckert, W., Mort, K., Jope, J., 1976, "Aerodynamic Design Guidelines and Computer Program for Estimation of Subsonic Wind Tunnel Performance," National Aeronautics and Space Administration, Washington.